Virus Evolution, 2025, **11(1)**, veae112
DOI: https://doi.org/10.1093/ve/veae112
Advance Access Publication 14 December 2024
Research Article

Major change in swine influenza virus diversity in France owing to emergence and widespread dissemination of a newly introduced H1N2 1C genotype in 2020

Gautier Richard[1,‡], Séverine Hervé[1,‡], Amélie Chastagner[1,‡], Stéphane Quéguiner[1], Véronique Beven[2], Edouard Hirchaud[2], Nicolas Barbier[1], Stéphane Gorin[1], Yannick Blanchard[2], Gaëlle Simon[1,*]

[1]ANSES, Ploufragan-Plouzané-Niort Laboratory, Swine Virology Immunology Unit, National Reference Laboratory for Swine Influenza, BP53, Ploufragan 22440, France
[2]ANSES, Ploufragan-Plouzané-Niort Laboratory, Viral Genetic and Biosecurity Unit, BP53, Ploufragan 22440, France

[‡]These authors contributed equally to this work.
*Corresponding author. ANSES, Ploufragan-Plouzané-Niort Laboratory, Swine Virology Immunology Unit, National Reference Laboratory for Swine Influenza, BP53, Ploufragan, 22440, France. E-mail: gaelle.simon@anses.fr

Abstract

Swine influenza A viruses (swIAVs) are a major cause of respiratory disease in pigs worldwide, presenting significant economic and health risks. These viruses can reassort, creating new strains with varying pathogenicity and cross-species transmissibility. This study aimed to monitor the genetic and antigenic evolution of swIAV in France from 2019 to 2022. Molecular subtyping revealed a marked increase in $H1_{av}N2$ cases from 2020 onwards, altering the previously stable subtypes' distribution. Whole-genome sequencing and phylogenetic analyses of $H1_{av}$ (1C) strains identified 10 circulating genotypes, including 5 new genotypes. The most predominant genotype from 2020 onwards, denominated $H1_{av}N2$#E, was characterized by an HA-1C.2.4, an N2-Gent/84, and internal protein-encoding genes belonging to a newly defined subclade within the Eurasian avian–like (EA) lineage termed EA-DK. $H1_{av}N2$#E emerged in Brittany, the country's most pig-dense region, and rapidly became the most frequently detected swIAV genotype across France. This drastic change in the swIAV lineage proportions at a national scale was unprecedented, making $H1_{av}N2$#E a unique case for understanding swIAV evolution and spreading patterns. Phylogenetic analyses suggested an introduction of the $H1_{av}N2$#E genotype from a restricted source, likely originating from Denmark. It spread rapidly with low genetic diversity at the start of the epizootic in 2020, showing increasing diversification in 2021 and 2022 as the inferred population size grew and stabilized, and exhibited reassortments with other enzootic genotypes. Amino acid sequence alignments of $H1_{av}N2$#E antigenic sites revealed major mutations and deletions compared to commercial vaccine 1C strain (HA-1C.2.2) and previously predominant $H1_{av}N1$ strains (HA-1C.2.1). Antigenic cartography confirmed significant antigenic distances between $H1_{av}N2$#E and other 1C strains, suggesting that the new genotype has escaped the pre-existing immunity of the swine population. Epidemiologically, the $H1_{av}N2$#E virus exhibited epizootic hallmarks with more severe clinical outcomes compared to $H1_{av}N1$ viruses. These factors likely contributed to the spread of $H1_{av}N2$#E within the pig population. The rapid rise of $H1_{av}N2$#E highlighted the dynamic nature of swIAV genetic and antigenic diversity, underscoring the importance of tailored surveillance programs to support risk assessment during potential new outbreaks. It also demonstrates the need to strengthen biosecurity measures when introducing pigs into a herd, including swIAV positivity assessment followed by quarantine, and restrict the trade of swIAV-excreting live swine between European countries.

Keywords: swine influenza; virus evolution; genetic diversity; epizootic; H1N2; surveillance; Eurasian avian–like lineage

Introduction

Swine influenza A virus (swIAV) infections are common in pig herds worldwide and typically cause an acute respiratory syndrome characterized by coughing, sneezing, nasal discharge, fever, and apathy lasting 5–7 days (Janke 2013, Vincent et al. 2014, Ma 2020). The disease can persist within a farm, contributing to the porcine respiratory disease complex and causing significant animal health issues and economic losses. SwIAV are of a One Health concern (Short et al. 2015) considering their zoonotic potential due to their ability to bind to α(2,6)-linked sialic acids (SAs) — the major influenza A virus (IAV) receptors in humans — and the weak immune cross-protection of the human popu-

lation against swIAV (Henritzi et al. 2020, Vandoorn et al. 2020). SwIAV also represents a risk for some avian species, especially turkeys, quails, and pheasants that also carry α(2,6)-linked SA, in addition to α(2,3)-linked SAs that are the receptors preferentially targeted by avian IAV (Choi et al. 2004, Massin et al. 2010, Starick et al. 2011, Bonfante et al. 2016). Pigs are susceptible to human and avian IAVs (Shinde et al. 2009, Zhang et al. 2020). As IAVs have a segmented RNA genome that allows genomic reassortment between strains when a host cell is coinfected, pigs have a capacity to generate reassortant IAVs, leading them to be described as "mixing vessel" hosts (Koçer et al. 2013, Nelson and Worobey 2018). Reassortment may occur between different swIAV strains cocirculating in pig populations, sometimes incorporating one or more alternate genes from human or avian IAVs. New reassortant viruses with genomic segments derived from multiple parental lineages may exhibit increased pathogenicity in pigs and/or intra- or interspecies transmission capacity (Koçer et al. 2013).

IAVs classify into subtypes based on antigenic differences in their two major surface glycoproteins, the hemagglutinin (HA) and the neuraminidase (NA). Three main subtypes, i.e. H1N1, H1N2, and H3N2, circulate in pigs, within which several lineages and whole-genome constellations are distinguished by geographical regions according to the history of their emergence (Vincent et al. 2014, Anderson et al. 2016). In 2016, a phylogeny-based global nomenclature classified the H1 viruses into three main clades (Anderson et al. 2016): Clade 1A grouping swIAVs with H1 from the so-called "classical swine lineage," including the 2009 pandemic H1 virus; Clade 1B grouping viruses with an H1 from human seasonal lineages ($H1_{hu}$); and Clade 1C grouping viruses with HA from the "Eurasian avian–like" (EA) lineage ($H1_{av}$). In Europe, three main lineages were described as enzootic in the European pig population in the early 2000: the "avian-like swine H1N1" ($H1_{av}N1$; HA-1C, N1) lineage, the "human-like reassortant swine H3N2" (H3N2; H3-1970.1, N2-Gent/84) lineage, and the "human-like reassortant swine H1N2" ($H1_{hu}N2$; HA-1B.1, N2-Scotland/94) lineage, all with internal protein-encoding genes (IGs, which encompass PB2, PB1, PA, NP, M, and NS) from the EA lineage. However, over the last 20 years, some major changes in the genetic diversity of European swIAVs have been reported: the emergence in 2003 in Denmark of an $H1_{av}N2$ reassortant, with Gent-like N2 and EA internal genes ($H1_{av}N2$), which has replaced the $H1_{hu}N2$ lineage in this country (Trebbien et al. 2013) and progressively spread in Germany (Zell et al. 2020), Spain (Portugal et al. 2021, Encinas et al. 2022), Italy (Chiapponi et al. 2021), and Bulgaria (Richard and Byrne 2024); the gradual decrease in the frequency of H3N2 virus in several countries (Simon et al. 2014, Henritzi et al. 2020; Portugal et al. 2021); the introduction of the 2009 pandemic H1N1 virus which has become the "pandemic-like swine H1N1" (H1N1pdm; HA-1A.3.3.2, $N1_{pdm}$) lineage, the fourth enzootic virus at the European level; and the emergence of numerous reassortant viruses containing one or more gene(s) from the H1N1pdm, which were sporadically detected or have been established locally, such as $H1_{pdm}N2$ viruses in UK, Germany, Spain, Italy, and Belgium (Parys et al., 2023, Simon et al. 2014, Anderson et al. 2016, Chiapponi et al. 2021, Encinas et al. 2022).

In a previous study which characterized swIAV genetic diversity in France from 2000 to 2018, we also showed an increase in the number of genotypes identified over time, despite very few H3N2 virus detections (Chastagner et al. 2020). However, the most dominant viruses characterized annually from 2010 to 2018 were $H1_{av}N1$ (min. 40%, max. 78%) and $H1_{hu}N2$ (min. 13%, max. 37%) lineages, both with EA internal segments, followed by H1N1pdm (min. 1%, max. 12%) (Chastagner et al. 2020). An $H1_{hu}N2$ antigenic variant ($H1_{hu}N2_{\Delta 146-147}$), which emerged in 2012 after having fixed mutations in epitopes and deletions in the receptor-binding site (RBS) on the HA gene, was detected increasingly until 2014 before being less prevalent among $H1_{hu}N2$ in following years. Until 2018, reassortant viruses remained sporadic but not rare. For instance, local $H1_{av}N1$ and $H1_{hu}N2$ viruses reassorted into $H1_{hu}N1$ and $H1_{av}N2$ (Chastagner et al. 2020), as well as $H1_{av}N1$ which reassorted with H1N1pdm, giving reassortants with various EA and/or pdm internal genes constellations (Henritzi et al. 2020). Contrary to other European countries, only two incursions of the Danish $H1_{av}N2$ virus with EA internal genes were reported in France in 2015, whereas another $H1_{av}N2$ of Denmark origin with H1N1pdm internal genes was identified once in late 2018 (Chastagner et al. 2020).

Given the ever-increasing genetic and antigenic diversity of swIAV, it is essential to continue to monitor their evolution in order to be able to conduct risk assessments of influenza infections in pigs, from both an animal health and public health perspective. In this study, we characterized the swIAVs detected in France through passive surveillance from 2019 to 2022 with a particular focus on viruses carrying an HA of the 1C clade. An epizootic took place in 2020 due to an $H1_{av}N2$ genotype that has drastically changed the frequencies of the swIAV subtypes previously established in France for years. This genotype resembled the Danish $H1_{av}N2$ strains previously identified sporadically in 2015. On the basis of genetic and antigenic data, we have reconstructed the evolutionary history of this newly dominant $H1_{av}N2$ virus and evaluated the determinants that would have helped its rapid and widespread dissemination in the pig population in France.

Material and methods

Samples, swine influenza A virus detection, and hemagglutinin/neuraminidase molecular subtyping

Nasal swabs (MW950Sent2mL Virocult®, Kitvia, Labarthe-Inard, France) were collected from January 2019 to December 2022 from pigs with acute respiratory disease in France thanks to the passive surveillance program implemented by Résavip (https://www.plateforme-esa.fr/fr/virus-influenza-porcins) (Hervé et al. 2019), diagnostic offers made by Ceva Santé Animale (Libourne, France) or requested by veterinarians, or epidemiological investigations conducted by the French Agency for Food, Environmental and Occupational Health & Safety (ANSES, Ploufragan, France). The Résavip network alone covered 207 different farms in 2019, 272 in 2020, 238 in 2021, and 200 in 2022, spanning 9 out of the 13 administrative regions of metropolitan France. In parallel with the sampling, the veterinarians collected outbreak-related information about the sampling date, the herd type, the vaccination program, the age and/or physiological stage of the sampled animals, the influenza-like illness intensity, and the epidemiological pattern of the outbreak.

Nasal swab supernatants were first screened in local veterinary laboratories for the presence of swIAV genome using M-gene real-time quantitive polymerase chain reaction (RT-qPCR) from two commercial kits validated by the French National veterinary Reference Laboratory (NRL) for Swine Influenza (ANSES, Ploufragan, France) (Pol et al. 2011). Then, swIAVs were subtyped by the NRL or LABOCEA22 (Ploufragan, France) using RT-qPCR assays specific to HA and NA genes of swIAV lineages known to circulate in France in 2018 ($H1_{av}$, $H1_{hu}$, $H1_{pdm}$, H3, N1, $N1_{pdm}$, and N2), as previously

described (Bonin et al. 2018). A new RT-qPCR assay was developed to specifically target HA-1C.2.4 of $H1_{av}N2$#E strains (see at the end of the Material and methods section for the RT-qPCR assay and see the Results section for the genotype description).

Swine influenza A virus sequencing

Viral RNA was extracted using the NucleoSpin® RNA Kit (Macherey-Nagel, Düren, Germany) directly from nasal swab supernatants or after virus propagation on Madin–Darby Canine Kidney (MDCK) cells according to standard procedures (Chastagner et al. 2020). All genomic segments of swIAV were amplified simultaneously before sequencing with the SuperScript III one-step RT-PCR system (Thermo Fisher Scientific, Waltham, MA, USA) using the universal IAV primers (Zhou et al. 2009). The nucleotide sequences were obtained by next-generation sequencing (NGS) on Thermo Fisher Scientific's Ion Proton instrument (Thermo Fisher, Carlsbad, CA, USA). The reads were cleaned using Trimmomatic v0.36, assembled into contigs using Spades, which were subsequently compared to an IAV database obtained from the National Center for Biotechnology Information (NCBI) using megablast to find reference sequences for each segment, on which the sequenced reads were mapped using BWA v0.7.15-r1140. The resulting BAM files were used to call consensus sequences using Influenza Sequences Toolbox v0.5 callConsensus tool (Richard 2024), which is notably based on seqkit (Shen et al. 2016) and samtools consensus (Danecek et al. 2021) with the following parameters "-t :hiseq –het-scale 0.42 –low-MQ 9 –scale-MQ 1.15." The NGS raw data obtained in this study have been made available in NCBI Bioproject PRJNA623701. Only consensus sequences of the complete genome were deposited in Genbank, and identification numbers are reported in Supplementary Table S1. If the consensus sequence did not cover the entire coding sequence, the segment was considered as partially sequenced and the strain genome as incomplete. Sequences from incomplete genomes were used for genotyping when they presented enough informative loci and are available upon request.

Swine influenza A virus genotyping

In addition to molecular subtyping, the genetic lineage of each genomic segment was determined by using a Basic Local Alignment Search Tool (BLAST) strategy implemented in the Influenza Sequences Toolbox v0.5 genotypeFasta tool (Richard 2024). This tool used BLAST to compare the obtained strain sequences to an in-house hand-curated database that is continuously incremented with data from swIAV strains identified in France since 2000, which is available upon specific request. For each gene, the best BLAST hit genotyping result was compared to the following seven best hits to verify the best-hit genotype consistency. The full-genome genotype and final FASTA files were then called for each strain using the Influenza Sequences Toolbox v0.5 annotateFasta tool, based on an in-house curated genotypes database and samples metadata database. The attributed HA genotypes were further confirmed by using the Bacterial and Viral Bioinformatics Resource Center webserver HA subspecies classification tool using the Orthomyxoviridae—Swine Influenza H1 global classification (https://www.bv-brc.org/app/SubspeciesClassification). The consistency of the attributed genotypes was assessed for all segments using maximum-likelihood phylogenies (see below).

Maximum-likelihood phylogenetic analyses

All publicly available swIAV sequences were collected from the Global Initiative on Sharing All Influenza Data and NCBI databases, and name duplicates were removed. All sequences were genotyped using the aforementioned genotyping pipeline, and only the strains displaying an HA from the 1C clade were kept for further analyses. Alignments and phylogenies were performed to determine the European strains that were closely related to the strains collected from France since 1990 by removing the poor-quality sequences (displaying consecutive stretches of >10 N) and using MAFFT (Katoh and Standley 2013), IQ-Tree (Minh et al. 2020), and FigTree (https://github.com/rambaut/figtree/releases). European strains located in the phylogeny in branches that displayed French strains were kept for further analyses. A detailed phylogeny (Supplementary Fig. S1) computed using IQ-Tree2 with the options "-bb 1000 -alrt 1000 -m GTR + F + I + G4" displays all available European HA-1C sequences as of September 2023 with colors corresponding to the ones that were kept or removed for further analyses. Phylogenies were performed using Nextstrain CLI v8.0.1 with default parameters by combining the filtered publicly available 1C European strains, the publicly available French 1C strains, as well as all 1C 2019-2022 French strains, for which a metadata table was built to store the following information: strains collection date, full-genome genotype, per gene clade, country, and location in France. In more detail, the sequences were filtered compared to the sequence metadata table using augur filter. Sequences were then aligned using augur align, and poor-quality sequences were then manually inspected and removed. Maximum-likelihood divergence trees were built using augur tree, based on IQ-Tree ultrafast bootstraps, with the following parameters "–override-default-args –substitution-model GTR+G4+F+I –tree-builder-args = "-bb 1000 -nt 8 -redo"." The substitution model was determined as being adapted to the analyzed datasets by using the IQ-Tree ModelFinder. Time-based phylogenies were subsequently built using augur refine, based on the metadata table and resulting divergence trees with the "–timetree –date-confidence –max-iter 30" option, based on the TreeTime algorithm (Sagulenko et al. 2018). The joint N1 N2 phylogenies root node date has been manually edited to reach the oldest N1 or N2 common ancestor (CA) date for visualization purposes of time-resolved trees. The resulting phylogenies and associated metadata were finally stored in a json file using augur export v2. The resulting auspice Nextstrain instances were then made available online: https://nextstrain.org/community/gtrichard/swIAV-H1av-France-2019-2022. The final phylogeny plots were made by extracting vector graphics from the Nextstrain instances and by further modifying them using Inkscape.

Bayesian phylogenetic analyses

Bayesian Evolutionary Analysis Sampling Trees (BEAST v1.10.4) was used to assess the country of origin of various CAs in the HA-1C.2.1, HA-1C.2.4, N2, and full-genome phylogenies (Suchard et al. 2018). Uncorrelated relaxed clock models were used to assess the trees internal branches rate of evolution using TreeStats v1.10.4. BEAST was also used to reconstruct the viral population size of the $H1_{av}N1$#A and $H1_{av}N2$#E strains collected in France between 2019 and 2022 (see the Results section for the description of the genotypes), using the Gaussian Markov Random Field (GMRF) Skyride model and computation in Tracer (Minin et al. 2008). Supplementary Table S2 describes the different BEAST runs, chain length, number of trees, models, datasets, and main traces Effective Sample Size (ESS, i.e. the number of effectively independent draws from the posterior distribution that the Markov chain is equivalent to) values.

Swine influenza A virus genotype distribution over time and space

The distribution of the genotyped viruses over the regions of France from 2019 to 2022 displayed as pie charts over the France map was generated using the sf, ggplot2, and dplyr R packages as well as the France regions GeoJSON (https://france-geojson.gregoiredavid.fr/repo/regions.geojson). Time-resolved metadata frequency plots representing genotypes proportions over time were generated by extracting exact dates of sampling (already known or inferred by the phylogeny) from the time-resolved HA phylogeny by using a custom jq command-line. The distribution of the genotyped viruses over time was then assessed using 2-month windows from 2019 to 2022 using streamgraph (https://github.com/hrbrmstr/streamgraph) with monotone interpolation, lubridate, and dplyr R packages.

Analysis of predicted amino acid sequences of the hemagglutinin- and neuraminidase-encoding genes

Predicted amino acid sequences of HA and NA from studied strains were obtained using AliView with standard genetic code and were aligned to the sequences described in the relevant figures, notably in order to compare the residues present on RBS and antigenic sites previously described in the literature. Amino acid frequencies and chemical properties were then represented using the ggseqlogo R package (Wagih and Hancock 2017).

Antigenic characterization

Swine antisera against swIAV strains representative of European enzootic lineages were produced in specific pathogen-free (SPF) pigs at ANSES Ploufragan-Plouzané-Niort facilities, as previously described (Chastagner et al. 2018). Four reference strains were used: A/swine/Cotes d'Armor/0388/09 ($H1_{av}N1$, HA-1C.2.1), A/swine/Cotes d'Armor/00186/10 ($H1_{av}N2$, HA-1C.2.1), A/swine/France/65-150242/2015 ($H1_{av}N2$, HA-1C.2.4), and A/swine/France/35-200154/2020 ($H1_{av}N2$, HA-1C.2.4). In addition, an antiserum against vaccine strains was produced by collecting blood of a vaccinated SPF sow 1 week after farrowing (Cador et al. 2016). The gilt was primo-vaccinated 6 and 3 weeks before insemination followed by three boosters 6, 3, and 2 weeks before farrowing with 2 ml of intramuscular injection of the inactivate trivalent vaccine Respiporc® Flu3 (IDT BIOLOGIKA GmbH, Dessau-Rosslau, Germany) comprising the following strains: A/swine/Haseluenne/IDT2617/2003 ($H1_{av}N1$, HA clade 1C.2.2, N1-EA, IG-EA), A/swine/Bakum/IDT1769/2003 (H3N2, N2-Gent/84, IG-EA), and A/swine/Bakum/1832/2000 ($H1_{hu}N2$, HA-1B.2.1, N2-Scot/94, IG-EA).

Hemagglutination inhibition (HI) assays were performed according to standard procedures (WOAH, 2023). Briefly, four hemagglutinating units (HAU) of MDCK-propagated virus were incubated with two-fold dilutions (starting at dilution 1:10) of the selection of swine antisera and tested against 0.5% chicken red blood cells. HI antibody titers were expressed as the reciprocal of the highest dilution inhibiting 4 HAU of virus. An antigenic cartography was performed using the Racmacs package to visualize the antigenic relationships between the swIAV strains isolated in France in 2019–2022, as well as to quantify the antigenic distances between antigens and sera. Briefly, the HI table was loaded in RStudio and a first map was made using the make.acmap function with 1000 optimizations. Unstable antigens according to Racmacs were discarded from further analyses, and a new antigenic map was built with 1000 optimizations using the dimension annealing option. Antigen and sera group information was added using the agFill and srFill functions. The bootstrapMap function was then used with 1000 repeats using the Bayesian method without reoptimization, from which bootstrapBlobs were computed. The final antigenic map and bootstrap variations were then represented. Distances from antigens to sera were extracted with the mapDistances function, while the antigenic distance from antigens to antigens was extracted by using the Euclidian distance within the antigenic map space. These distributions of the distances expressed in Antigenic Units (AU) were then represented as boxplots using ggplot2.

Design of $H1_{av}$#E RT-qPCR assay specific to the $H1_{av}N2$#E genotype

Nucleotide sequence alignments of HA-1C.2 genes from representative strains of $H1_{av}$ (HA-1C) lineage revealed that $H1_{av}N2$#E strains (see the Results section for the genotype description) from 2020 fixed deletions of three and six nucleotides, giving rise to the loss of three amino acids at positions 137, 146, and 147 after the methionine, respectively, as compared to $H1_{av}$ sequences from ancestral enzootic Clade 1C.2.1, which made them unique compared to other $H1_{av}$ sequences identified in France, including those from $H1_{av}N2$#E strains of 2015 and from the $H1_{av}N2$#F strains (Supplementary Fig. S2, see the Results section for the genotype description). A pair of primers and a TaqMan probe have thus been designed based on these HA gene sequence alignment analyses: Fw tttcccaaagaactcatggc, at position 399–418 from the first nucleotide of the HA coding sequence MW048844; Rv gaataaggttttcccttgcttg (497–518); and probe FAM-cgggaacaacagtttcatgctccaa-BHQ1 (431–455).

The RT-qPCR assays were run using the MX3005P instrument (Stratagene, Agilent Technologies, La Jolla, CA, USA). Each PCR mixture contained 5 µl of RNA extract and 20 µl of master mix composed of 2× GoTaq Probe qPCR Master Mix, 1× GoScript RT Mix for one-step RT-qPCR (Promega, Fitchburg, WI, USA) as well as 800 nM of each primer and 300 nM of probe. The cycling conditions used were 15 min of reverse transcription at 45°C, 2 min of denaturation at 95°C, and 42 cycles of 15 s at 95°C and 1 min at 58°C.

Several panels incorporating virus strains and/or clinical samples were constituted to evaluate the performance of the developed RT-qPCR (Supplementary Table S3). Analyses showed 100% analytical specificity. Evaluation of analytical sensitivity indicated that the assay would be able to detect equivalent to around 35 Cq-values based on in-house M-gene RT-qPCR. Analyses of viral RNA from nasal swab supernatants previously identified by HA/NA RT-qPCR and sequencing showed 100% [95% confidence interval (CI): 87.66%–100%] of diagnostic specificity and 96.55% (95% CI: 82.24%–99.91%) of diagnostic sensitivity with only one false-negative sample, probably due to the low amount of genome target.

Statistical analyses

Statistical analyses were performed using R 3.4.0. For epidemiological data, the difference in proportion between groups was tested using the following method: based on $H1_{av}N1$ and $H1_{av}N2$ positive samples, considering one epidemiological category (for instance physiological stage of pigs), $H1_{av}N2$#E (see the Results section for the genotype description)-infected animal numbers were compared to $H1_{av}N1$-infected animal numbers for a given epidemiological category (breeding versus the rest) by assembling a 2×2 contingency table and by using the epitools R package riskratio function (Aragon 2020). This returned for each

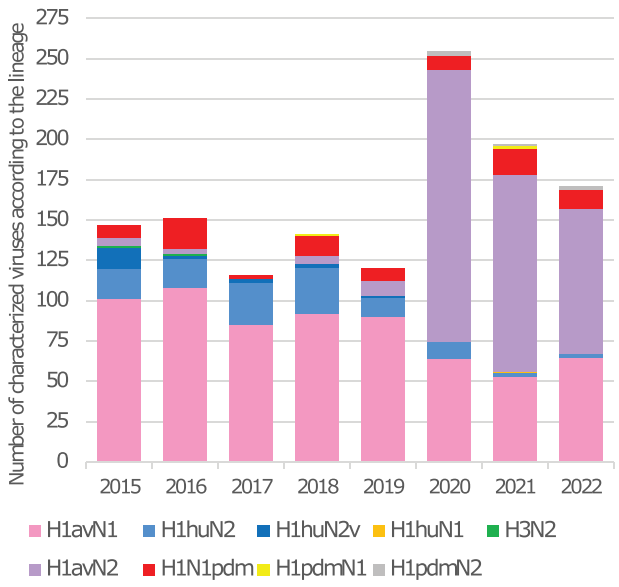

Figure 1. Numbers of swIAV strains identified in France from 2019 to 2022 using PCR subtyping, per year, according to their subtype, and comparison to numbers previously reported from 2015 to 2018 (Chastagner et al. 2020).

comparison the χ^2 test *P*-value as well as the risk ratio estimate and 95% CI upper and lower bounds of one epidemiological category for $H1_{av}N2$- versus $H1_{av}N1$-infected animals. For antigenic data comparison, the means of HI antibody titers obtained by groups of strains were log2-transformed and compared with a Wilcoxon rank-sum test using R 3.4.0 (wilcox.test).

Results

Molecular subtyping of swine influenza A viruses detected in France in 2019–2022

In 2019, 387 independent respiratory outbreaks were investigated in pig herds in France, a number similar to the mean annual number (405 ± 57) of farms investigated from 2015 to 2018 (Hervé et al. 2019). By contrast, this number has risen sharply in 2020, as 661 outbreaks were investigated. The proportions of outbreaks confirmed to be swIAV positive by M-gene RT-qPCR in 2019 and 2020 (47.3% and 52.6%, respectively) were similar to the average annual proportion of 48.2 ± 3.7% calculated in 2015–2018 (Hervé et al. 2019). Among the 531 cases of swIAV-infected herds detected in 2019–2020, 375 (70.6%) swIAV strains were fully HA/NA subtyped by specific RT-qPCRs. In 2019, 120 strains were identified as follows: 90 $H1_{av}N1$ (HA-1C, 75%), 13 $H1_{hu}N2$ (HA-1B, 10.8%) including 1 $H1_{hu}N2_{\Delta 146\text{-}147}$ variant, 8 H1N1pdm (HA-1A, 6.7%), and 9 $H1_{av}N2$ (HA-1C, 7.5%), and no H3 viruses were detected (Fig. 1). Compared to the distributions reported from 2015 to 2018 (Chastagner et al. 2020), which showed quite stable numbers and proportions in the different H1 lineages over time, the proportion of $H1_{hu}N2$ has halved, the $H1_{av}N2$ proportion tripled, whereas other subtype frequencies remained equivalent. In 2020, 255 virus strains were fully subtyped, i.e. twice more than in previous years when 116–150 strains were identified per year. Intriguingly, the proportions of the different subtypes were completely shuffled, with 168 $H1_{av}N2$ (HA-1C, 65.9%), 64 $H1_{av}N1$ (HA-1C, 25.1%), 11 $H1_{hu}N2$ (HA-1B, 4.3%), 9 H1N1pdm (HA-1A, 3.5%), and 3 $H1_{pdm}N2$ strains (HA-1A, 1.2%).

In 2021, the swIAV passive surveillance reached 727 respiratory outbreaks and 307 (42.2%) positive cases. Among them, 197 swIAV strains were subtyped and distributed as follows: 122 $H1_{av}N2$ (HA-1C, 61.9%), 53 $H1_{av}N1$ (HA-1C, 26.9%), 16 H1N1pdm (HA-1A, 8.1%), 2 $H1_{hu}N2$ (HA-1B, 1%), 2 $H1_{pdm}N1$ (HA-1A, 1%), 1 $H1_{hu}N1$ (HA-1B, 0.5%), and 1 $H1_{pdm}N2$ (HA-1A, 0.5%) (Fig. 1). In 2022, the situation was quite similar to 2021 and 2020, with, however, fewer cases investigated (548 outbreaks, 45.3% of positive cases). The $H1_{av}N2$ remained the most prevalent strain ($n = 90$, 52.6%, HA-1C), followed by 65 $H1_{av}N1$ (37.8%, HA-1C) and 12 H1N1pdm (7%, HA-1A). $H1_{hu}N2$ remained low ($n = 2$, 1.2%, HA-1B), and two $H1_{pdm}N2$ (1.2%, HA-1A) were detected.

Phylogenies, genotyping, and spatiotemporal distribution of 2019–2022 1C swine influenza A virus

The diversity and phylogeny of these newly emerging and persisting $H1_{av}N2$ viruses were then characterized by monitoring the evolution of swIAV displaying an HA gene of the 1C clade. Swine IAV strains collected from 2019 to 2022 were submitted to whole-genome sequencing. After genotyping, 331 swIAV genome sequences displayed an HA of the 1C clade and were analyzed using maximum-likelihood phylogenies, when sequence quality permitted, alongside related European sequences that were publicly available at the time of September 2023 (Fig. 2). For HA, clades 1C.2.1, 1C.2.2, or 1C.2.4 were detected, and the N1-EA, N2-Gent/84, N2-Scotland/94, and human seasonal-N2 clades were detected for the NA segment (Fig. 2a). Three clades were distinguished for all six IGs: EA, EA-DK, and pdm (Fig. 2b). The EA-DK subclade was newly established in this study considering its important evolutionary distance compared to the EA lineage for all IG. The name EA-DK was given as sequences from Denmark were predominant in the root of this new subclade (Supplementary Fig. S3).

Overall, 10 full-genome genotypes were identified among 1C strains collected between 2019 and 2022 in France (Fig. 3a). Regarding $H1_{av}N1$ subtype, four genotypes were distinguished: genotype $H1_{av}N1$#A (HA-1C.2.1, N1-EA, IG-EA) continued to be predominant in 2019 (Fig. 3a and b) and across the entire country (Fig. 3c). Both genotypes $H1_{av}N1$#B (HA-1C.2.1, N1-EA, and IG-EA-DK) and $H1_{av}N1$#D (HA-1C.2.1, N1-EA, and IG-EA with M-EA-DK), which had never been detected in France before, were sporadic and found only in the western part of France throughout the 2020–2022 period (Fig. 3b and c). Genotype $H1_{av}N1$#C (HA-1C.2.2, N1-EA, IG-EA) was also sporadically reported at the end of 2019 in the "Hauts-de-France" region and throughout 2022 in "Hauts-de-France" and "Auvergne-Rhône-Alpes" regions (Fig. 3b and c).

Within the $H1_{av}N2$ subtype, six genotypes were identified (Fig. 3a). The $H1_{av}N2$#A (HA-1C.2.1, N2-Scotland/94, and IG-EA) used to be sporadically detected almost every year since 2008 following a reassortment between local enzootic $H1_{av}N1$#A and $H1_{hu}N2$ viruses (Chastagner et al. 2020). However, only five $H1_{av}N2$#A strains were detected in Brittany in 2019 and 2020. The vast majority of the sequenced $H1_{av}N2$ strains belonged to the $H1_{av}N2$#E (HA-1C.2.4, N2-Gent/84, and IG-EA-DK) (Fig. 3a). This genotype started to be detected sporadically at the beginning of 2020 to rapidly become the most detected genotype, especially in Brittany, the French region with the highest density of pig farming. It was then detected in seven out of the nine monitored administrative regions of the country and maintained as the most detected strain for the rest of the study period, thus replacing $H1_{av}N1$#A as the predominant genotype (Fig. 3b). The other $H1_{av}N2$ genotypes were sporadic just like the $H1_{av}N2$#A. Five strains belonged to the $H1_{av}N2$#F genotype (HA-1C.2.4, N2-Gent/84, and IG-pdm) (Fig. 3a) and were reported in Brittany in 2019 and 2020. It was

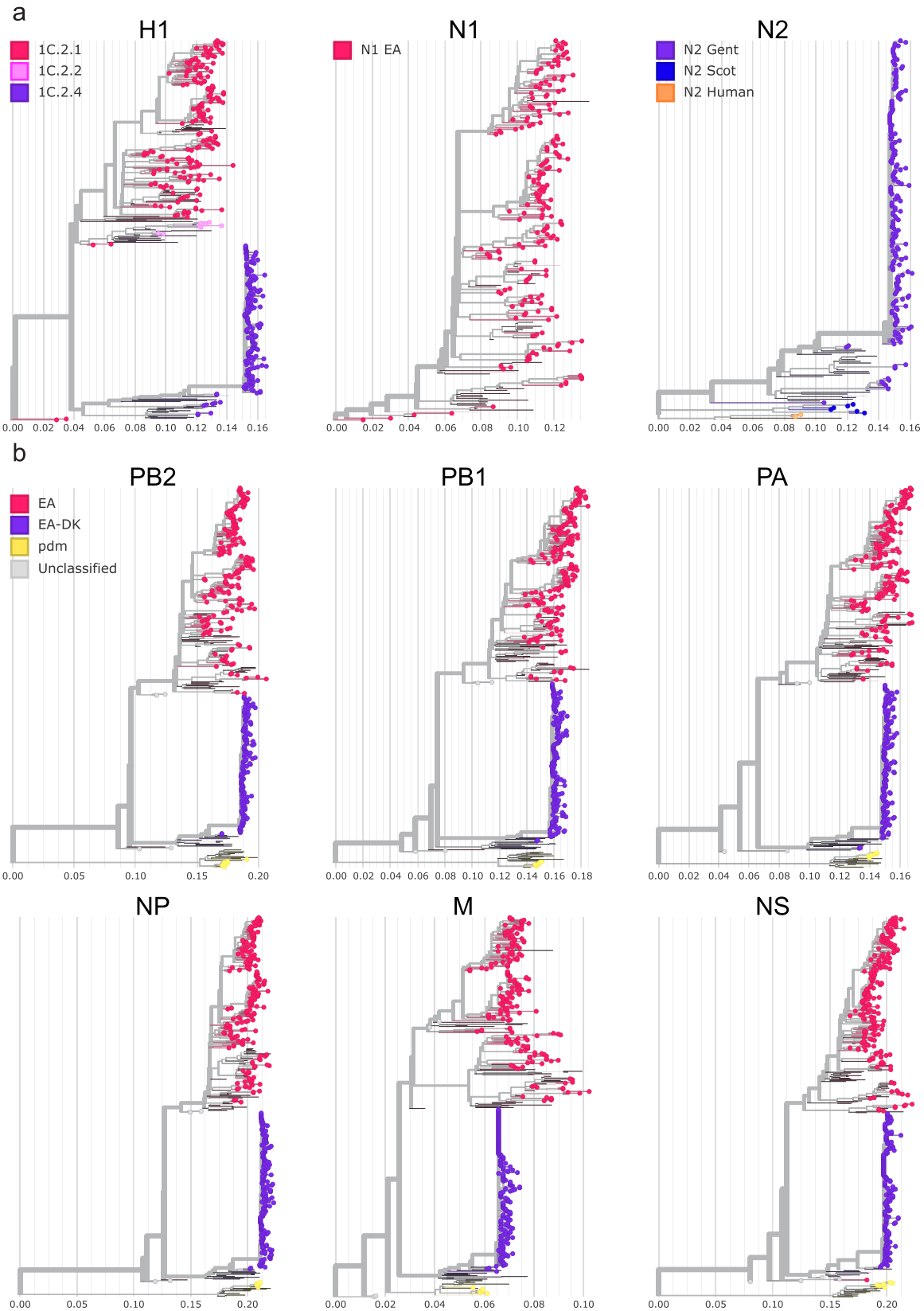

Figure 2. Maximum-likelihood divergence phylogenies of the eight segments of swIAVs collected and sequenced in France from 1992 to 2022 having an HA of the 1C (EA) clade and the related publicly available European sequences. (a) Surface protein-encoding genes phylogenies (H1, N1, and N2). (b) IG phylogenies (PB2, PB1, PA, NP, M, and NS). Sequences are represented by dots colored according to their individual segment clade: EA in pink, Eurasian avian–like Denmark (EA-DK) in purple, Pandemic09 in yellow (pdm). Publicly available European sequences as of September 2023 are displayed as thin branches without dots. Interactive versions of the trees can be found at https://nextstrain.org/community/gtrichard/swIAV-H1av-France-2019-2022.

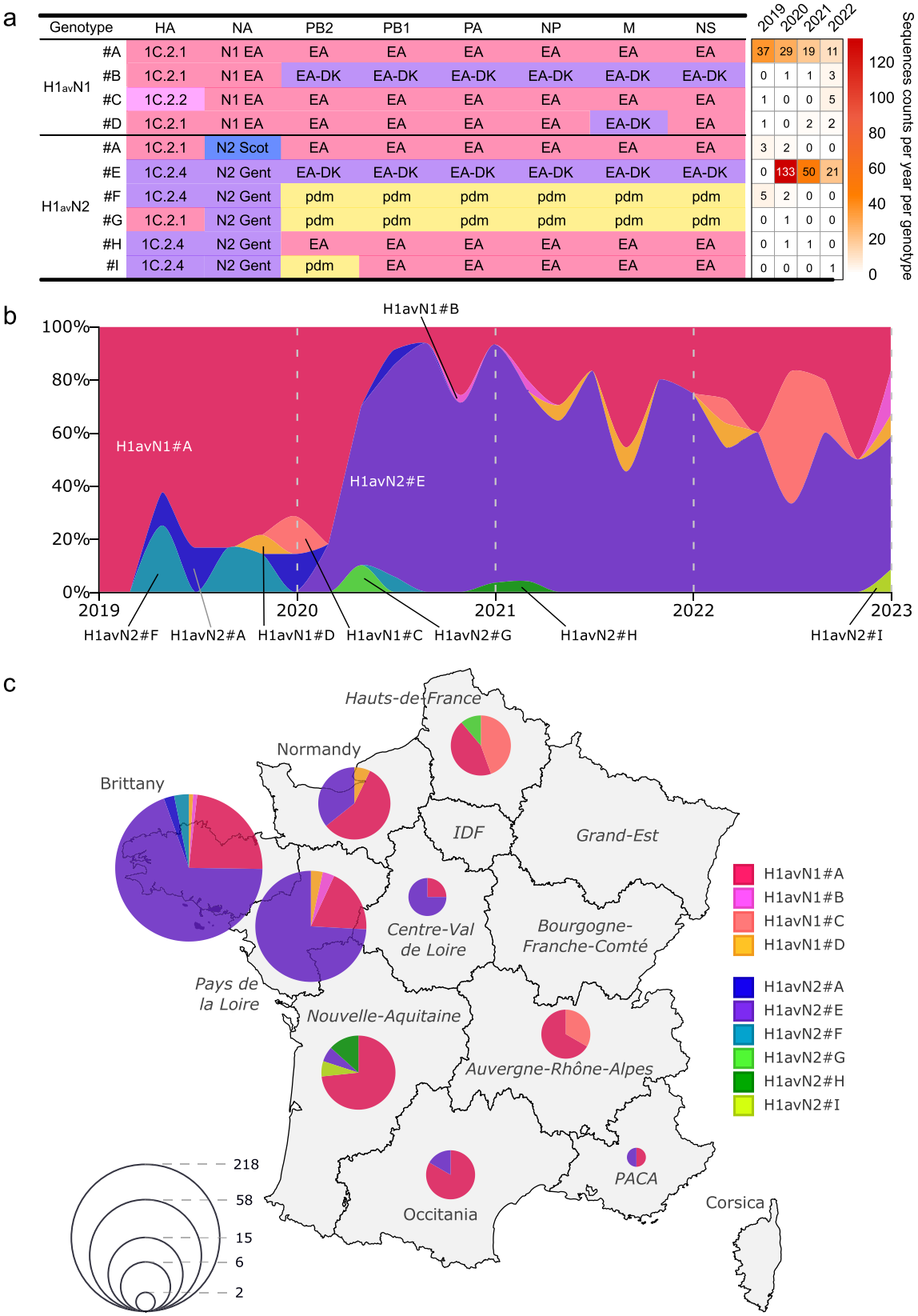

Figure 3. Spatiotemporal distribution of 1C swIAV genotypes identified in France from 2019 to 2022. (a) Details of the gene constellation of the 10 swIAV HA-1C genotypes. The counts of full-genome sequences collected each year are displayed as a heatmap, for each genotype, on the right side of the table. (b) Normalized bimestrial country-wide proportion of the swIAV genotypes. (c) Region-resolved map of France. Each pie chart represents the proportions of swIAV genotypes identified in the associated region between 2019 and 2022. The size of the pie chart is proportional to the log2 number of sequences collected. Abbreviations: IDF, Ile-de-France; PACA, Provence-Alpes-Côte-d'Azur.

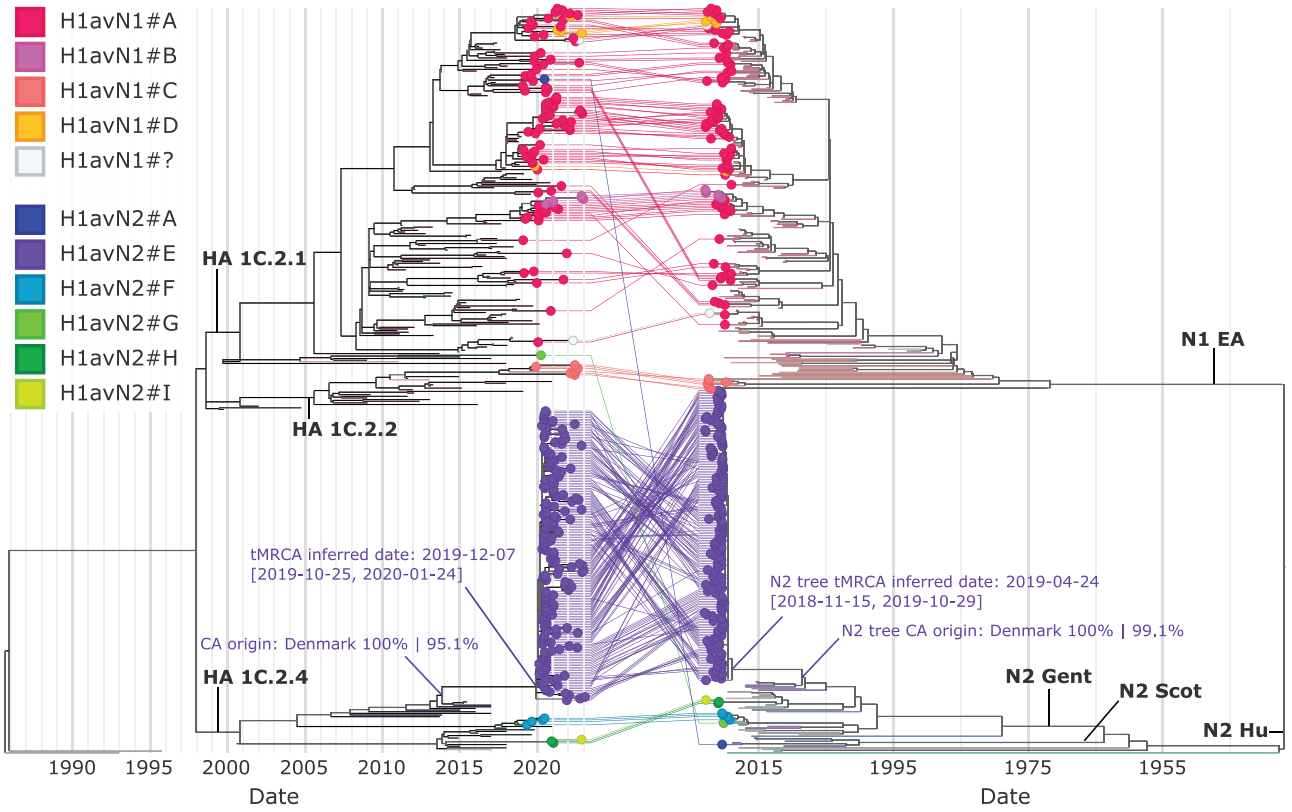

Figure 4. Time-resolved maximum-likelihood phylogenies of the surface protein-encoding genes (left: HA, right: NA) colored by genotypes as presented in Fig. 3. Dots represent swIAV sequences collected in France between 2019 and 2022. Branches without dots represent publicly available European 1C swIAV strains as of September 2023, including previous strain sequences collected in France. Central lines connect the HA and NA sequences of the same strains. $H1_{av}N1$ strains with missing internal genes sequences are indicated as "$H1_{av}N1$#?" Inferred date and CI are displayed for the $H1_{av}N2$#E 2020–2022 clade CA in both HA and NA trees. The probable country of origin of the CA is indicated with the first number corresponding to the country.prob calculated by BEAST, and the second number corresponds to the TreeTime migration test value (both phylogenies were matching). An interactive version of the tree can be found at https://nextstrain.org/community/gtrichard/swIAV-H1av-France-2019-2022/HA:community/gtrichard/swIAV-H1av-France-2019-2022/NA?c=genotype&f_country=France.

first detected in November 2018 in Brittany (Chastagner et al. 2020) and was suggested to be introduced *in toto* from abroad, likely from Denmark considering the HA/NA and full-genome phylogenies of the newly sequenced $H1_{av}N2$#F strains (Supplementary Fig. S4a, CA origin is 100% Denmark with BEAST and 48.1% Denmark with TreeTime for HA and 81% Denmark with BEAST and 96% France with TreeTime for NA; Supplementary Fig. S5, CA origin is 96.7% Denmark with BEAST and 44.2% Denmark with TreeTime). Three $H1_{av}N2$ genotypes were detected for the first time during the study period: $H1_{av}N2$#G (HA-1C.2.1, N2-Gent/84, IG-pdm) which corresponded to a single strain detected in March 2020 in the "Hauts-de-France" region; $H1_{av}N2$#H (HA-1C.2.4, N2-Gent/84, and IG-EA), which was detected only twice in the "Nouvelle-Aquitaine" region in December 2020 and January 2021; and a single strain similar to $H1_{av}N2$#H but with a PB2 from the pdm lineage, detected in the same region at the end of 2022 and got designated as belonging to the $H1_{av}N2$#I genotype (Fig. 3).

Origins of the newly detected sporadic swine influenza A virus genotypes

Throughout this study, five swIAV genotypes were detected for the first time in France and their potential origins were checked through maximum-likelihood HA/NA tanglegram (Fig. 4) and whole-genome phylogenies as well as BEAST and TreeTime migration test. The $H1_{av}N1$#B and $H1_{av}N1$#D strains, considering that their HA and NA phylogenies were confounded within the $H1_{av}N1$#A phylogenies, were most likely reassortants between this genotype and H1avN2#E from which they acquired one or more EA-DK IG (Fig. 4). $H1_{av}N1$#B circulated for ~2 years and a half between 18 July 2020 [(1 July 2020–18 July 2020), inferred time to Most Recent Common Ancestor] and 20 December 2022 (last detection). It formed a single phylogenetic cluster according to HA and NA phylogenies, thus likely corresponding to a single reassortment event (Fig. 4). Meanwhile, the $H1_{av}N1$#D reassortant seemed to have formed at three different occasions independently according to both HA and NA phylogenies, with the earliest sequence detected in 30 October 2019 and the latest sequence detected in 18 November 2022.

The $H1_{av}N2$#G strain displayed an HA from Danish origins (99.9% probability from BEAST and 97.3% from TreeTime, Supplementary Fig. S4b) and an NA gene close to both Danish and French strains according to BEAST and TreeTime analyses (Supplementary Fig. S4b). Full-genome alignments of $H1_{av}N2$#F strains showed a high probability of origin from Denmark (Supplementary Fig. S5, 96.7% using BEAST and 44.2% using TreeTime), which thus suggested that the $H1_{av}N2$#G strain was likely an $H1_{av}N2$#F reassortant on the HA gene (HA-1C.2.4 was replaced by HA-1C.2.1) introduced *in toto* from abroad, likely from Denmark.

The $H1_{av}N2$#H and $H1_{av}N2$#I strains were not related to any already sequenced strain from France but clustered with sequences found in Denmark and Italy for both HA and NA (Supplementary Fig. S4c). This suggested an introduction *in toto* from

abroad of the $H1_{av}N2\#H$ strain. The most recent CA displayed an origin from Denmark at 100% for both HA and NA using both BEAST and TreeTime. Considering the HA/NA phylogeny, the #I genotype was most likely a reassortant of the #H genotype on the PB2 segment (EA to pdm). The reassortment might have happened in France considering how close the two strains are on the HA and NA genes as well as considering that they were detected sequentially in the same region of the country.

Origins of the newly predominant $H1_{av}N2\#E$ swine influenza A virus genotype

Genotyping of the 1C viruses revealed that the $H1_{av}N2\#E$ genotype was solely responsible for the rise of the $H1_{av}N2$ detections during the 2020–2022 period. Such a contrasted and fast switch of the mainly detected swIAV genotypes at the scale of France was unprecedented. This raised the question of the potential origins of these $H1_{av}N2\#E$ strains.

The $H1_{av}N2\#E$ genotype formed a single phylogenetic cluster, whose inferred date of the last CA was estimated to be set between October 2019 and January 2020 according to Nextstrain analyses of the HA gene, while the analyses on the NA gene had CI spanning over a year between November 2018 and October 2019 (Fig. 4). Before 2020, only two $H1_{av}N2\#E$ isolates were characterized in the south-western part of France in 2015 (Chastagner et al. 2020). The $H1_{av}N2\#E$ genotype was thus not detected from 2016 to 2019, until its identification in Brittany in February 2020. HA/NA phylogenies indicated that the $H1_{av}N2\#E$ 2020 strains detected in France were related to 2017–2018 sequences detected in Europe (Fig. 4) and that the most recent CA with European strains had an origin from Denmark at ~100% using BEAST and TreeTime for both HA and NA. Full-genome phylogeny of all $H1_{av}N2\#E$ strains confirmed that the strains detected in France in 2020 were closer to strains from Denmark identified from 2015 to 2017 than to the French 2015 strains (Fig. 5a). Amino acid conservation analyses confirmed that most IGs of a representative $H1_{av}N2\#E$ 2020 strain were closer to 2015–2017 strains from Denmark than to the A/swine/France/65-150242/2015 strain, while HA and NA were equally similar (Fig. 5b).

Further analyses of the HA gene phylogeny by measuring the branches length (divergence) showed that $H1_{av}N2\#E$ HA diversity was quite low in 2020 and significantly increased overtime in 2021 and 2022, while HA divergence within $H1_{av}N1\#A$ remained stable over the same period (Fig. 6a). The evolution of $H1_{av}N2\#E$ overtime happened at a constant rate of evolution just like the $H1_{av}N1\#A$ genotype according to BEAST analyses using an uncorrelated relaxed clock model (Fig. 6b), with 3.30e–3 substitutions per site per year for $H1_{av}N2\#E$ strains and 3.93e–3 for $H1_{av}N1\#A$ strains. The independent reconstruction of the viral population size using BEAST GMRF Skyride models and analyses on the 2019–2022 $H1_{av}N1\#A$ and $H1_{av}N2\#E$ sequences confirmed the epizootic phase of the $H1_{av}N2\#E$ genotype from the end of 2019 to the start of 2020, followed by an enzootic phase. Interestingly, a decrease in the $H1_{av}N1\#A$ population size seemed concomitant with the $H1_{av}N2\#E$ epizootic start (Fig. 6c). No seasonality patterns were observed.

Taken together, this suggested that $H1_{av}N2\#E$ strains were introduced *in toto* from abroad, possibly from Denmark, from a limited number of entry points at the end of 2019 considering the low diversity of the $H1_{av}N2\#E$ in 2020, as well as the single group structure of the $H1_{av}N2\#E$ 2020 phylogeny. It then continued to evolve at a constant rate of evolution.

Antigenic characterization of $H1_{av}N2\#E$ strains

In order to better understand how the $H1_{av}N2\#E$ strains spread so rapidly over the country, their antigenic properties were compared to those of long-established $H1_{av}N1\#A$ strains, as well as vaccine related strains (HA-1C or N2 antigens).

HA and NA antigenic sites as well as HA RBS of the $H1_{av}N2\#E$ collected in France from 2020 to 2022 ($n = 177$, called $H1_{av}N2\#E \geq 2020$) were aligned (Fig. 7a) with (i) $H1_{av}N2\#E$ strains found in Denmark and France up to 2017 ($n = 6$, called $H1_{av}N2\#E \leq 2017$, Fig. 5 star-annotated sequences); (ii) the HA-1C.2.2 and N2 sequences of strains included in the Respiporc® Flu3 vaccine (Ceva Santé Animale, France), the only commercial vaccine currently available in Europe with a 1C antigen; and (iii) with $H1_{av}N1\#A$ strains collected during the study period ($n = 84$). This analysis first revealed a low diversity of the antigenic sites and RBS among the $H1_{av}N2\#E \geq 2020$ (Fig. 7a, first row), as only two positions (HA 239 E or K, NA 334 N or K) displayed more than one amino acid with the alternative forms represented over 10% among the 177 analyzed sequences. While this suggested stable antigenic properties of the $H1_{av}N2\#E$ strains collected over the study period, the E239K mutation was found more prominently in 2021–22 than in 2020 (21/25 sequences, χ^2 $P = 1.4e{-}3$), highlighting the HA-1C.2.4 diversification overtime at the antigenic level. By contrast, compared to the other analyzed sequences (Fig. 7a, first row compared to others), the $H1_{av}N2\#E \geq 2020$ strains displayed many amino acid mutations involving chemical properties change in the HA and NA antigenic sites as well as RBS (Fig. 7a, orange arrow-annotated positions). This included a deletion at Position 146 in the RBS and the overlapping Sa HA antigenic site, thus forming a 146–147 double deletion compared to the $H1_{av}N1\#A$ strains and 1C.2.2 vaccine strain. Taken together, these mutations would predict differences in antigenic properties of the $H1_{av}N2\#E$ strains compared to the 1C vaccine strain as well as to the previously predominant $H1_{av}N1\#A$ strains.

Antigenic distances between $H1_{av}N2\#E$ strains, $H1_{av}N1$ strains, and vaccine antigens were measured in HI tests using two anti-HA-1C.2.1 hyperimmune sera (HIS), one anti-2015 HA-1C.2.4 serum, one anti-2020 HA-1C.2.4 serum, and one post-vaccination serum (PVS) containing anti-HA-1C.2.2 antibodies (Table 1, Supplementary Fig. 6). The $H1_{av}N2\#E$ 2020 reference antigen and $H1_{av}N2\#E$ strains collected in 2020–2022 reacted properly with the anti-2020 HA-1C.2.4 serum (HI titers of 1280 and 584 on average, respectively), while the reaction was much lower with the anti-2015 HA-1C.2.4 serum (HI titers of 160 and 107 on average, respectively) and little to no cross-reaction was detected with the anti-HA-1C.2.1 $H1_{av}N1$ serum (HI titers of 20 and 41 on average, respectively) and with the PVS (HI titers of 10 and 20 on average, respectively). The HA-1C.2.1 reference antigens as well as the HA-1C.2.1 and HA-1C.2.2 strains detected in the study period ($H1_{av}N1\#A$ and #C, respectively) did not cross-react with the anti-2020 HA-1C.2.4 serum and only slightly with the anti-2015 HA-1C.2.4 serum, while they reacted well with the PVS (Table 1). The differences in HI test results evidenced between $H1_{av}N1$ and $H1_{av}N2\#E$ strains were significant for all antisera (Supplementary Fig. S6), which highlighted the inability of anti-HA-1C.2.1 sera and PVS to recognize $H1_{av}N2\#E \geq 2020$ strains antigens.

An antigenic cartography was built using HI titers of HA-1C.2.4, 1C.2.1, and 1C.2.2 strains against anti-2015 HA-1C.2.4, anti-2020 HA-1C.2.4, anti-HA-1C.2.1 sera, and the PVS (Fig. 7b). HA-1C.2.4 antigens displayed consistent antigenic distances between

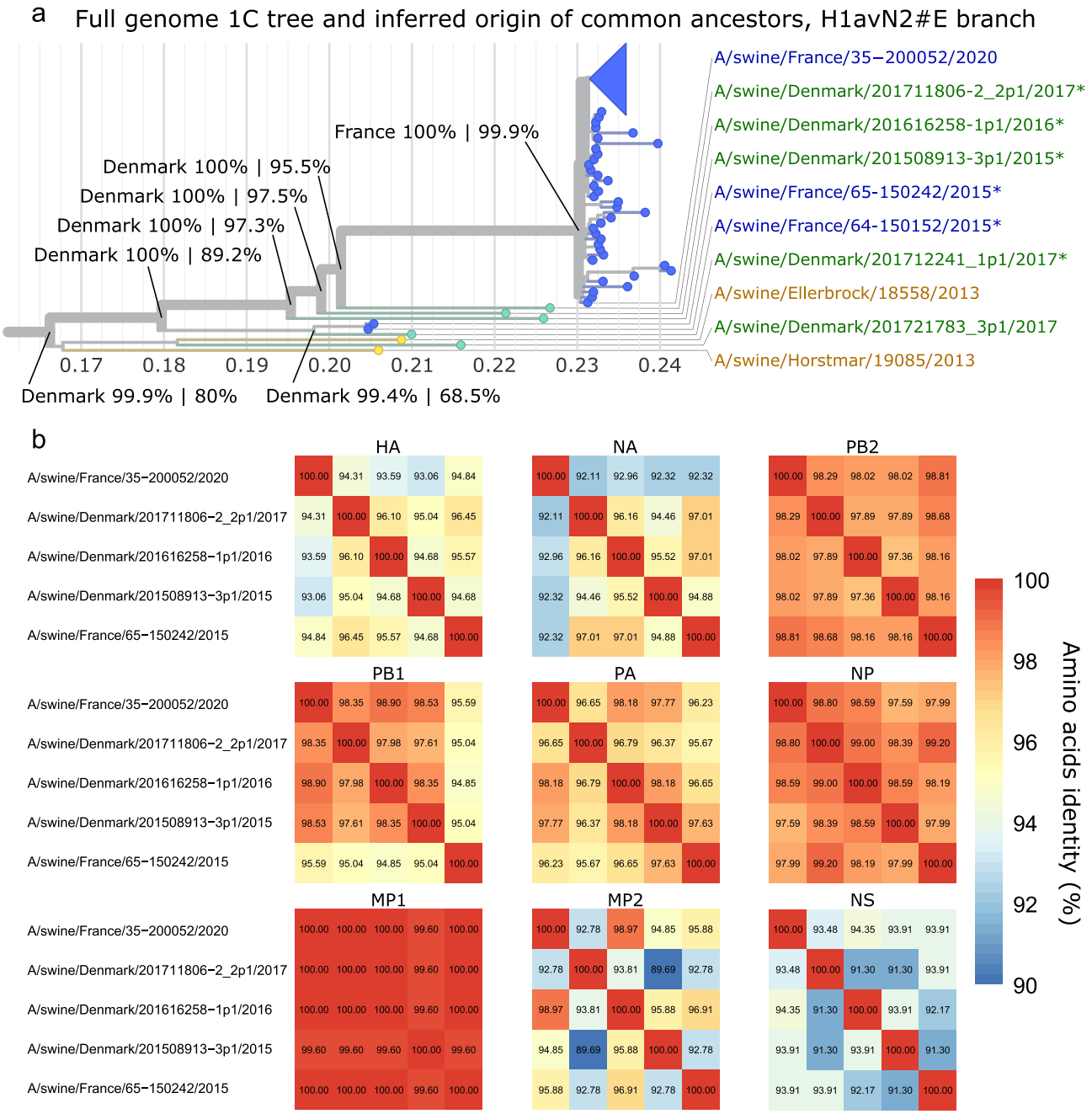

Figure 5. Probable origins of the $H1_{av}N2\#E$ viruses detected in France from 2020 to 2022. (a) Left: $H1_{av}N2\#E$ viruses branch of the full-genome maximum-likelihood divergence tree of the 1C swIAV strains in France and Europe. Right: name of the publicly available European sequences, as of July 2024, that are the most closely related to the $H1_{av}N2\#E$ viruses detected in France. The probable country of origin of the sequences CAs is indicated, the first number corresponds to the country.prob calculated by BEAST, and the second number corresponds to the TreeTime mugration test value (both phylogenies were matching). The A/swine/France/35-200 052/2020 corresponds to the $H1_{av}N2\#E$ detected in France that is the closest to pre-2020 sequences. Sequences annotated by stars represent the $H1_{av}N2\#E$ publicly available sequences closest to the $H1_{av}N2\#E$ collected in France during the 2020–2022 period. (b) Amino acid identity comparison of the sequences of nine proteins of the A/swine/France/35-200 052/2020 strain and the closest pre-2020 European $H1_{av}N2\#E$ strains.

each other, with a median of 1.28, but a median antigenic distance of 4.27 and 4.78 units when compared to HA-1C.2.1 and HA-1C.2.2 antigens, respectively (Supplementary Fig. S7). These differences were found significant (Wilcoxon rank-sum test P-value < 1.13e−10). The same was observed when measuring antigen-to-serum distances (Fig. 7c): HA-1C.2.4 strains displayed significant antigen–serum distances over 4 (Wilcoxon rank-sum test P-values < 1.8e−4) for both anti-HA-1C.2.1 serum (9.80-fold cross-reactivity loss, Table 1) and PVS (4.45-fold cross-reactivity loss, Table 1) when compared to HA-1C.2.1 and HA-1C.2.2 strains, which displayed nonsignificant median distances below 2 AU (Wilcoxon rank-sum test P-values > .17) (Fig. 7c). Taken together, the newly predominant $H1_{av}N2\#E$ strains displayed significant (Barr et al. 2014, Lewis et al. 2016, Centers for Disease Control and Prevention 2022) antigenic distances with HA-1C.2.1 and HA-1C.2.2 strains, as well as with the PVS.

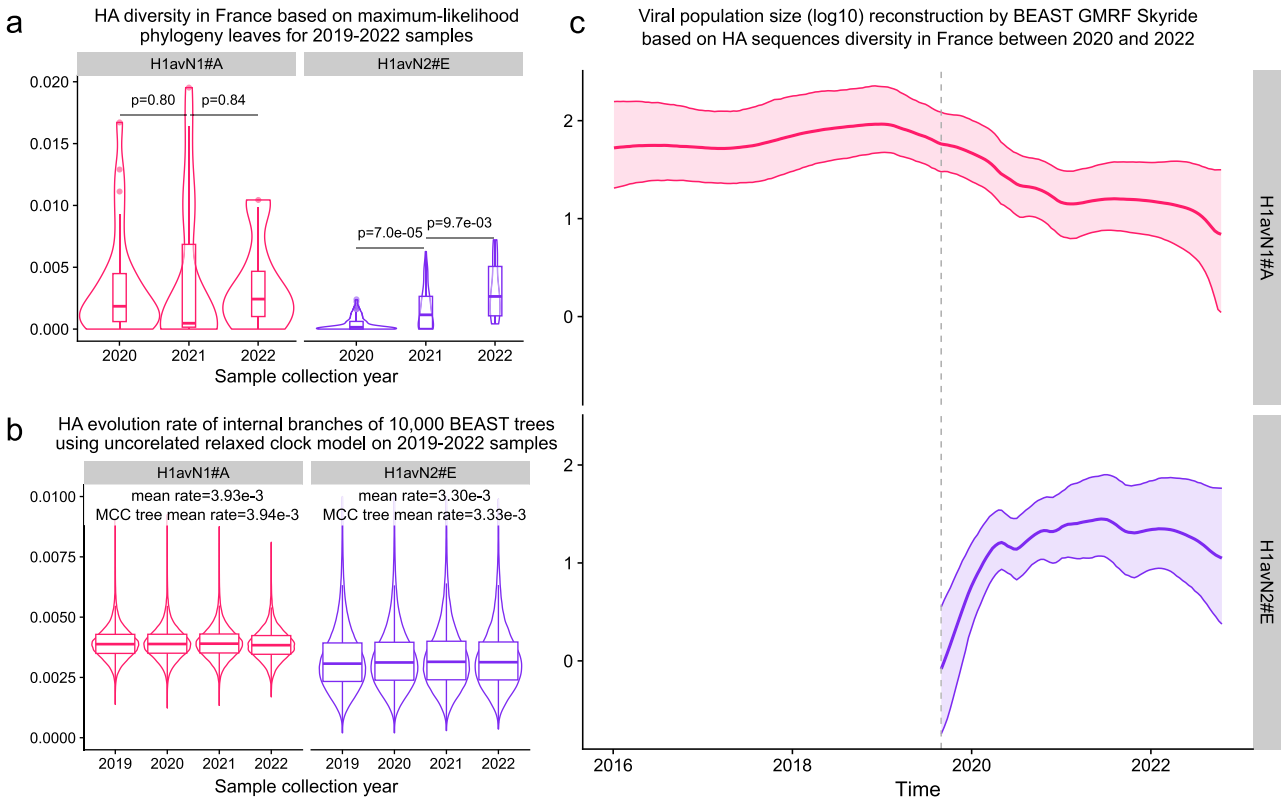

Figure 6. Evolution patterns of the newly spreading $H1_{av}N2$#E (purple) viruses compared to the long-established $H1_{av}N1$#A (pink) viruses in France across the 2019–2022 period. (a) Distribution of the HA divergence phylogeny leaves length for $H1_{av}N1$#A and $H1_{av}N2$#E viruses collected between 2020 and 2022 in France, displayed as superposed boxplots and density plots. Wilcoxon rank-sum test P-values compare the distributions between the virus genotypes. (b) Distribution of the rates of evolution of the HA gene per year assessed through BEAST using the uncorrelated relaxed clock model on the internal branches of 10 000 trees. (c) Independent viral population size reconstructions, expressed in log10, assessed by BEAST GMRF Skyride analysis based on the HA diversity across 10 000 trees.

Epidemiology of the $H1_{av}N2$#E outbreaks

Owing to the detection rate of swIAV strains belonging to the emerging $H1_{av}N2$#E genotype in 2020, we aimed to rapidly discriminate them within $H1_{av}$ (Clade 1C.2) strains following the initial HA/NA molecular subtyping step. Thus, we developed a Taqman RT-qPCR assay targeting a specific region of the HA-1C.2.4 segment of the $H1_{av}N2$#E strains, an assay which displayed 100% analytical and diagnostic specificity and 96.55% diagnostic sensitivity (see Material and methods section).

This new HA-1C.2.4-gene RT-qPCR led to the identification of 352 cases of infection by an $H1_{av}N2$#E virus from 2020 to 2022. Epidemiological data collected at the time of pig sampling in those affected herds were compared to those collected in the 272 herds that were found infected by $H1_{av}N1$ strains (HA-1C.2.1) during 2 periods of time, i.e. 2019–2020 and 2021–2022. When comparing the outbreaks caused by $H1_{av}N2$#E and $H1_{av}N1$ viruses, no difference was found concerning their repartition within the different types of farms (Table 2). During the early period of the epizootic (2019–2020), $H1_{av}N2$#E cases were more often associated with sporadic acute infection ["classical form," Relative Risk (RR)= 1.93 (1.53–2.43), 77.4% versus 45.7%, χ^2 $P = 3.5e{-}8$] and clinical signs more severe than the norm [RR = 1.50 (1.15–1.95), 50% versus 30.9%, χ^2 $P = 1.6e{-}3$] compared to $H1_{av}N1$ cases which displayed recurrent infection patterns with moderate clinical signs (Table 2). No differences between both groups were significant when comparing the form and the clinical intensity of the outbreaks that occurred in 2021–22. $H1_{av}N2$#E infections were reported in pigs of all physiological stages just like $H1_{av}N1$ viruses. However, during the early period of epizootic, the proportion of piglets infected before 10 weeks of age was weaker in $H1_{av}N2$#E than in $H1_{av}N1$ outbreaks [RR = 0.66 (0.51–0.85), χ^2 $P = 7.4e{-}4$], while the proportions of growing pigs (≥10 weeks) were similar in both groups. The proportion of breeding animals infected by $H1_{av}N2$#E was higher than those infected by $H1_{av}N1$ [RR = 2.99 (1.58–5.64), 24.3% versus 5.5%, χ^2 $P = 7.2e{-}6$]. A total of 75.4% of $H1_{av}N2$#E-infected gilts and sows were hosted in farms that applied mass or batch-to-batch vaccination programs with the Respiporc® Flu3 trivalent vaccine. When only considering infected breeders, more $H1_{av}N2$#E outbreaks were reported in vaccinated farms than $H1_{av}N1$ in 2021–22 [RR = 3.53 (1.63–7.69), χ^2 $P = 6.7e{-}4$]. However, no significant differences were found in the distribution of outbreaks in vaccinated farms based on the detection of infected animals of all physiological stages.

Discussion

The surveillance of swIAVs organized in France since the 2009 pandemic and the in-depth characterization of the strains, notably thanks to the Résavip surveillance network, allowed us to regularly monitor their genetic and antigenic evolution. Subtyping, sequencing, and phylogenetics and the compilation of related epidemiological data helped answering questions concerning the etiology of cases of acute respiratory syndromes and have led to the development of new diagnostic tools to adapt to swIAV genetic diversification. From 2019 to 2022, when compared to the previous

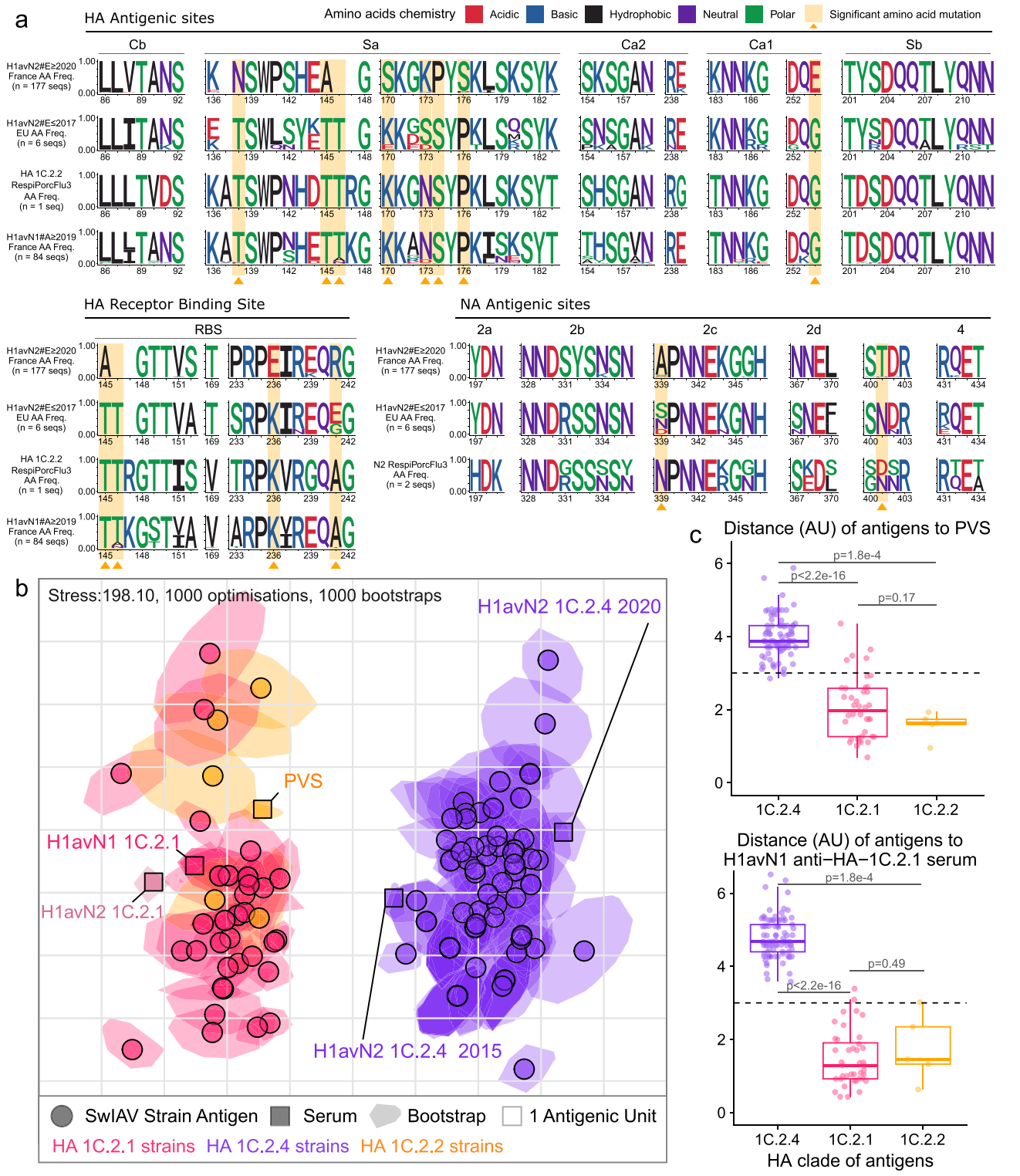

Figure 7. Antigenic properties of the $H1_{av}N2$#E viruses detected in France between 2020 and 2022. (a) Amino acid motifs of the HA/NA antigenic sites and HA RBSs. Frequency of amino acids found for each position was calculated across the 177 HA or NA $H1_{av}N2$#E sequences (top line), the 6 HA or NA $H1_{av}N2$#E sequences detected in France and Denmark before 2020 (second line, stars annotated sequences in Fig. 5), for the HA of the 1C.2.2 antigen contained in the Respiporc® Flu3 vaccine (third line), or for the $H1_{av}N1$#A HA-1C.2.1 sequences collected in France between 2019 and 2022 (fourth line). Mutations between the top line and the other lines leading to changes in chemical properties are highlighted by an orange background and arrow. (b). Antigenic map based on HI test results presented in Table 1 and Supplementary Fig. S6. Virus strains detected in France from 2019 to 2022 are displayed as circles: HA-1C.2.1 ($H1_{av}N1$#A) in pink, HA-1C.2.2 ($H1_{av}N1$#C) in orange, and HA-1C.2.4 ($H1_{av}N2$#E) in purple. Five sera are displayed as squares: anti-HA-1C.2.4 toward 2015 and 2020 viruses in purple, anti-HA-1C.2.1 toward 2009 ($H1_{av}N1$ in pink) and 2010 ($H1_{av}N2$ in pale pink) viruses, and one PVS (Respiporc® Flu3 trivalent commercial vaccine) in orange. Vertical and horizontal axes are expressed in AU (Racmacs after 1000 optimizations). Variations across 1000 bootstraps are displayed as shadowed area around each dot. (c) Antigenic distance distributions between strains and antisera of each HA clade, measured from the antigenic map and displayed as boxplots with the median as a bold line. Wilcoxon rank-sum test P-values are represented above the compared distributions. Antigen to antigen distances distributions are represented in Supplementary Fig. S7

Table 1. Cross-HI data obtained for $H1_{av}N1$ and $H1_{av}N2\#E$ viruses against HIS and post-vaccination serum (PVS) produced in SPF pigs.

			HI titers to HIS produced against selected isolates				PVS produced against
			$H1_{av}N1$	$H1_{av}N2$	$H1_{av}N2$	$H1_{av}N2$	®Respiporc Flu3 $H1_{av}N1$, $H1_{hu}N2$, H3N2 antigens
Subtype	HA clade	swIAV strains	CA/0388/2009 Anti-HA-1C.2.1	CA/0186/2010 Anti-HA-1C.2.1	65-150242/2015 Anti-2015 HA-1C.2.4	35-200154/2020 Anti-2020 HA-1C.2.4	Anti-HA-1C.2.2
$H1_{av}N1$	1C.2.1	A/Sw/France/29-200272-01/2020	1280	640	160	10	160
$H1_{av}N2$	1C.2.1	A/Sw/Cotes d'Armor/0186/2010	640	640	40	80	160
$H1_{av}N2$	1C.2.4	A/Sw/France/65-150242/2015	80	10	1280	10	20
$H1_{av}N2$	1C.2.4	A/Sw/France/35-200154/2020	20	10	160	1280	10
$H1_{av}N1$ (1C.2.1 or 1C.2.2) strains from 2019 to 2022			**402** (40–1280) ($n = 67$)	**168** (<10–640) ($n = 67$)	**46** (<10–320) ($n = 67$)	**16** (<10–40) ($n = 29$)	**89** (20–320) ($n = 44$)
$H1_{av}N2\#E$ (1C.2.4) strains from 2020 to 2022			**41*** (<10–160) ($n = 94$)	**13*** (10–40) ($n = 94$)	**107*** (20–320) ($n = 94$)	**584*** (80–1280) ($n = 38$)	**20*** (10–80) ($n = 94$)
$H1_{av}N1/H1_{av}N2\#E$			**9.8**	**12.92**	**0.43**	**0.03**	**4.45**
$H1_{av}N2\#E/H1_{av}N1$			**0.1**	**0.08**	**2.33**	**36.5**	**0.23**

The table reports the HI titers for reference antigens (homologous HI titers are underlined). Then, the geometric mean HI of each group of tested strains is indicated in bold, significant difference (*T*-test *P*-value < .05) between the two groups is pointed by an asterisk, the range of HI antibody titers obtained within each group is reported in square brackets, and the number of tested strains in brackets. The last two lines indicate the cross-reactivity fold-change for each serum by calculating the ratio between the HI titer geometric means of $H1_{av}N2\#E$ and $H1_{av}N1$ strains.
*Wilcoxon rank-sum test *P*-value < .05 for comparison between log2 HI titer distribution of $H1_{av}N2\#E$ and $H1_{av}N1$ (1C.2.1 or 1C.2.2) strains. The distribution plots and exact *P*-values are displayed in Supplementary Fig. S6.

2000–18 period (Chastagner et al. 2020), new $H1_{av}N2$ genotypes, i.e. $H1_{av}N2\#G$, #H, and #I and the reassortants $H1_{av}N1\#B$ and #D, have been characterized while remaining sporadic. More importantly, a new predominant $H1_{av}N2$ genotype was identified, the $H1_{av}N2\#E$, which was detected only sporadically in 2015 in the south-west of France but reappeared in the north-west in February 2020.

In 2020, the number of swIAV herd infection cases detected through passive surveillance has doubled compared to previous years, coinciding with the emergence of $H1_{av}N2\#E$ viruses which widely spread in the country. The $H1_{av}N2\#E$ took over the previously predominant $H1_{av}N1\#A$ according to our surveillance data and our Bayesian viral population size reconstruction analyses. Indeed, the $H1_{av}N2\#E$ likely got introduced at the end of 2019 in France with a rapid increase in the population size (epizootic phase) followed by a maintenance phase (enzootic phase), which coincided with a decrease in $H1_{av}N1\#A$ population size. $H1_{av}N2\#E$ quickly became the most frequently detected genotype, especially in Brittany, which accounted for 56.3% of the French pig population in 2020 in only 5% of the country's territory (IFIP—Institut du Porc 2023). The $H1_{av}N2\#E$ genotype was not related to viruses that were previously circulating in France and was found to be more similar to the enzootic Danish $H1_{av}N2$ viruses (Trebbien et al. 2013). The $H1_{av}N2\#E$ genotype exhibits an HA gene classified by OFFLU within HA-Clade 1C.2.4 among the 1C EA lineage (https://www.offlu.org/wp-content/uploads/2021/03/OFFLU-VCM-SWINE-FINAL3_to_be_Uploaded.pdf), a clade shared by other H1N2 viruses found in Denmark, Spain, Italy, and Bulgaria (Richard and Byrne 2024). Meticulous phylogenic analyses revealed that $H1_{av}N2\#E$ IGs could be classified as a new EA subclade that we named EA-DK considering the prevalence of Danish strains at the root of this clade. Most gene phylogeny for the $H1_{av}N2\#E$ genotype detected in France displayed a long branch, corresponding to unsampled diversity. This could not be solved by asking for unreleased sequences to European swIAV surveillance laboratories. However, three $H1_{av}N2$ strains from Denmark were closer to the $H1_{av}N2\#E$ strains when considering the entire IAV genome. Meanwhile, these Danish HA sequences shared a 94.3% identity with the earliest detected $H1_{av}N2\#E$ strain in 2020 in France, which was on par with the 94.8% HA identity of the 2015 $H1_{av}N2\#E$ strains detected in south-western France. These analyses combined with the identified epizootic pattern in the population size reconstruction led to hypothesize an introduction *in toto* from Denmark between November 2018 and January 2020, but considering the sparseness of the swIAV sampling in Europe, the virus could have transited to France from another European country. It is, however, important to note that France imported live pigs for rearing/breeding mainly from Denmark from 2019 to 2021 (Supplementary Figure S8).

In addition to this newly predominant $H1_{av}N2\#E$ virus, four sporadic $H1_{av}N2$ genotypes were detected during the study period. Three of them seemed to have been introduced *in toto* from foreign countries just like the $H1_{av}N2\#E$, i.e. $H1_{av}N2\#F$, $H1_{av}N2\#G$, and $H1_{av}N2\#H$. The introduction of these genotypes from abroad underscores the importance of testing animals for swIAV positivity before exportation to another country, as well as quarantining them in designated areas with appropriate biosecurity measures when entering intensive confined farms, regardless of their origin. Such adequate biosecurity measures should be adopted and applied at the European level to control swIAV spreading as efficiently as possible. Moreover, the circulation of additional viral genotypes in herds increases the risks of simultaneous infections by different IAVs, which can themselves lead to the emergence of new reassortant viruses (Chastagner et al. 2019). This threat was here illustrated by the detection of three new reassortant genotypes, i.e. $H1_{av}N1\#B$, $H1_{av}N1\#D$, and $H1_{av}N2\#I$, which likely formed on the territory from genotypes introduced from abroad. The impact of such reassortants on the evolution of swIAV strains in France cannot be predicted and this poses new challenges and threats considering their zoonotic potential and ability to infect other animal species.

Table 2. Distribution of swIAV-positive cases belonging either to $H1_{av}N2$#E (HA-1C.2.4) or to $H1_{av}N1$ (HA-1C.2.1) subtype according to epidemiological data recorded in infected farms. *: Results of χ^2 test *P*-value: <0.05.

	2019–2020		2021–2022	
	$H1_{av}N1$	**$H1_{av}N2$**	**$H1_{av}N1$**	**$H1_{av}N2$**
Type of production farm				
Farrowing-to/post-weaning (N, NPS)	7	13	9	24
Postweaning (PS)	1	1	0	1
Farrowing-to-finishing (NE)	104	113	87	135
Postweaning-finishing (PSE)	31	17	17	29
Finishing (E)	8	7	2	7
Epidemiological pattern of infection[a]				
Classical form	64	113*	71	112
Recurrent form	76	33	38	69
	P = 3.5e−8, RR = 1.93 (1.53–2.43)			
Severity of clinical signs[b]				
Moderate	94	63	63	108
High	42	63*	25	36
	P = 1.6e−3, RR = 1.50 (1.15–1.95)			
Physiological stage of pigs				
Piglets (<10 weeks)	96	67*	61	108
	P = 7.4e−4, RR = 0.66 (0.51–0.85)			
Growing (≥10 weeks)	41	42	35	54
Breeding	8	35*	17	30
	P = 7.2e−6, RR = 2.99 (1.58–5.64)			
Vaccination program[c]				
All physiological stages of infected animals				
Not vaccinated farm	70	61	62	88
Vaccinated farm	76	85	48	107
Only considering infected breeders				
Not vaccinated farm	2	11	11	4
Vaccinated farm	6	23	6	23*
			P = 6.7e−4, RR = 3.54 (1.63–7.69)	

[a]The "Classical" form is defined by a sporadic acute infection, and the "Recurrent" form is related to an endemic pattern of infection at the herd level, affecting each successive batch of pigs at a given physiological stage (Chastagner et al. 2020).
[b]The "Moderate" intensity of the disease is defined by clinical signs lasting no more than 2–3 days at the individual level and without mortality, while the "High" intensity form lasts longer than usual and/or can be associated with some mortality.
[c]Vaccination against swine influenza was only applied in breeding animals.

Since the emergence of the $H1_{hu}N2$ virus in 1994, which contributed to the disappearance of the H3N2 virus in north-western France (Gourreau et al. 1994, Brown et al. 1998, Simon et al. 2014), the $H1_{av}N2$#E virus is the first to drastically disrupt the relative proportions of swIAV lineages that circulated in France for 30 years. Such a diversity switch in the swIAV population at a national scale was unprecedented, and the collected sequencing data constitute a unique opportunity to follow the evolution of a newly spreading swIAV. Interestingly, $H1_{av}N2$#E displayed low diversity at the start of the epizootic in 2020 on their HA gene, suggesting a restricted source of introduction in France, and as time passed, their diversity increased. The emergence of such a virus remains unknown and only future sequence analyses will allow us to understand this virus evolution pattern. Comparatively, in 2009, despite the pressure of the H1N1pdm virus causing a pandemic in humans and a panzootic disease in pigs worldwide, French pig farms were weakly affected. The H1N1pdm virus failed to prevail against the enzootic $H1_{av}N1$ and $H1_{hu}N2$ viruses in north-western regions where they were well established (Chastagner et al. 2018). This context arose the question of the factors allowing a new swIAV genotype to emerge, become epizootic, and later, enzootic.

Several biotic and abiotic factors drive the becoming of an airborne virus, like influenza, to become epizootic after its emergence: (i) the density of sensitive host, i.e. the proportion of host population without pre-existing immunity (Rose and Madec 2002, te Beest et al. 2013) and (ii) the fitness/virulence of the virus which defines its ability to infect the host cells or prevail in the case of viral competition (Schrauwen and Fouchier 2014).

Concerning the proportion of a host population without pre-existing immunity, we showed in the present study that $H1_{av}N2$#E strains were significantly distant antigenically (above 4 AU) from HA-1C.2.1 strains, as well as from PVS Respiporc® Flu3 antigens. These results are consistent with those we reported in a previous study, where $H1_{av}N2$#E was efficiently neutralized by homologous antiserum, but not by anti-HA-1C.2.1 serum or PVS (Deblanc et al. 2024). In this previous study, we also reported that Respiporc® Flu3 vaccinated piglets were not fully protected from $H1_{av}N2$#E infection, whereas they were against $H1_{av}N1$#A under our experimental conditions (Deblanc et al. 2024). Contrastingly, H1N1pdm strains were shown to cross-react with anti-HA-1C.2.1 sera, and the antigenic distance between antigens was in that case below 3 (Lewis et al. 2016, Chepkwony et al. 2021). Overall, this suggested that $H1_{av}N2$#E viruses likely escaped the swine population's pre-existing immunity, either to the previously predominant $H1_{av}N1$#A swIAV or to the Respiporc® Flu3 vaccine and related strains, thus contributing to the rapid spread of the $H1_{av}N2$#E virus over the country, unlike H1N1pdm virus in 2009. The introduction of the $H1_{av}N2$#E virus in a high-density pig farming region such as Brittany also most likely contributed to the successful $H1_{av}N2$#E spread. This raises apprehension considering the intensification of the pig farming, with a stable decrease in the number of holdings, but an increase in or stabilization of the number of pigs since 2010 (IFIP—Institut du Porc 2023).

Concerning the virus fitness and ability to infect new hosts, this is often associated with the induced symptoms and viral shedding. The beginning of the $H1_{av}N2$#E epizootic was associated with a higher proportion of high-severity clinical signs in HA-1C.2.4 swIAV-infected animals compared to $H1_{av}N1$-infected animals. This is in accordance with our experimental results as we also showed that $H1_{av}N2$#E-infected animals displayed stronger and prolonged clinical signs compared to $H1_{av}N1$-infected ones (Deblanc et al. 2024). The $H1_{av}N2$#E strains thus appeared to be more virulent than $H1_{av}N1$ strains, at least before significant genetic evolution, which most likely contributed to their rapid spread and to the increase in the total number of swIAV outbreaks investigated in 2020 through the passive surveillance programs. Interestingly, the virulence of the $H1_{av}N2$#E outbreaks during the 2021–22 period was not significantly different from that of the $H1_{av}N1$ outbreaks. This suggests that a certain level of population immunity may have developed during the $H1_{av}N2$#E enzootic period.

To conclude, $H1_{av}N2\#E$ was detected as the new predominant swIAV genotype in France, and while some elements concerning their antigenic and virulence properties were studied, their airborne transmissibility and resistance in the environment to temperature or pH remain to be characterized and compared to the previously predominant $H1_{av}N1$ viruses (Sooryanarain and Elankumaran 2015). The pathway of introduction $H1_{av}N2\#E$ swIAVs to France from abroad as well as the spreading dynamics in France also remains to be elucidated. Phylogeographic analyses at the scale of France, and eventually Europe, linking precise geographic and sequence data of swIAV samples with animal movements and epidemiological data would help to characterize swIAV transmission pathways. Moreover, $H1_{av}N2\#E$ spread in France raises the question of potential spillovers of the genotype to other countries importing live pigs from France. To prevent new epizootics and the establishment of new enzootic viruses, it is crucial to prevent the introduction of new swIAV genotypes in herds by strengthening quarantine measures and encouraging the monitoring of swIAV infections in live swine traded, especially for breeding, both between and within European countries, as is done for other diseases (The European Commission 2019), even though swine influenza is not a regulated disease.

Acknowledgements

The authors are indebted to all farmers and veterinarians for their participation in influenza virus monitoring. They gratefully acknowledge all members of Résavip, the French national public–private network for surveillance of IAVs in pigs, especially regional coordinators as well as national partners involved in the dedicated swine influenza virus working group from the national platform for animal health epidemiosurveillance (https://www.plateforme-esa.fr/page/thematique-virus-influenza-chez-le-porc). They also thank Agnès Jardin *et al.*, Ceva Santé Animale (Libourne, France), for their contribution to pig sampling and first intention analyses. Thanks also go to Nicolas Rose *et al.*, from the Swine Epidemiological and Welfare Unit, ANSES (Ploufragan, France) for visiting pig herds and contribution to swIAV surveillance, as well as to Frédéric Paboeuf and colleagues from the SPF Pig Production and Experimentation Unit, ANSES (Ploufragan, France) for antiserum productions. Gautier Richard, Séverine Hervé, Stéphane Gorin, Stéphane Quéguiner, Nicolas Barbier, and Gaëlle Simon are members of the French research network on influenza viruses (ResaFlu; GDR2073) financed by the CNRS. Gautier Richard, Séverine Hervé, and Gaëlle Simon are members of the European Swine Influenza Network (ESFLU; COST action CA 21132).

Author contributions

G.S., G.R., S.H., and A.C. contributed to conceptualization; S.Q., N.B., S.G., E.H., and V.B. contributed to investigation; G.R., S.H., and A.C. contributed to formal analysis; G.R. and S.H. contributed to data curation and methods; G.R. contributed to visualization of the manuscript; G.R., S.H., A.C., and G.S. contributed to writing—original draft preparation; G.R., S.H., A.C., Y.B., and G.S. contributed to writing—review and editing; G.S. and S.H. contributed to the project administration. All the authors have read and agreed to the published version of the manuscript.

Supplementary data

Supplementary data is available at *VEVOLU Journal* online.

Conflict of interest: None declared.

Funding

None declared.

Data availability

The NGS raw data obtained in this study have been made available in NCBI Bioproject PRJNA623701. Only consensus sequences of complete genome were deposited in Genbank, and identification numbers are reported in Supplementary Table S1.

References

Anderson TK, Macken CA, Lewis NS *et al.* A phylogeny-based global nomenclature system and automated annotation tool for H1 hemagglutinin genes from swine influenza A viruses. *mSphere* 2016;**1**:e00275-16.

Aragon TJ. *epitools: Epidemiology Tools*. 2020. https://CRAN.R-project.org/package=epitools 15 September 2024, date last accessed.

Barr IG, Russell C, Besselaar TG *et al.* WHO recommendations for the viruses used in the 2013–2014 Northern Hemisphere influenza vaccine: epidemiology, antigenic and genetic characteristics of influenza A(H1N1)pdm09, A(H3N2) and B influenza viruses collected from October 2012 to January 2013. *Vaccine* 2014;**32**:4713–25.

Bonfante F, Fusaro A, Tassoni L *et al.* Spillback transmission of European H1N1 avian-like swine influenza viruses to turkeys: a strain-dependent possibility? *Vet Microbiol* 2016;**186**:102–10.

Bonin E, Quéguiner S, Woudstra C *et al.* Molecular subtyping of European swine influenza viruses and scaling to high-throughput analysis. *Virol J* 2018;**15**:7.

Brown IH, Harris PA, McCauley JW *et al.* Multiple genetic reassortment of avian and human influenza A viruses in European pigs, resulting in the emergence of an H1N2 virus of novel genotype. *J Gen Virol* 1998;**79**:2947–55.

Cador C, Hervé S, Andraud M *et al.* Maternally-derived antibodies do not prevent transmission of swine influenza A virus between pigs. *Vet Res* 2016;**47**:86.

Centers for Disease Control and Prevention. *Antigenic Characterization*. 2022. https://www.cdc.gov/flu/about/professionals/antigenic.htm (6 June 2024, date last accessed).

Chastagner A, Bonin E, Fablet C *et al.* Virus persistence in pig herds led to successive reassortment events between swine and human influenza A viruses, resulting in the emergence of a novel triple-reassortant swine influenza virus. *Vet Res* 2019;**50**:77.

Chastagner A, Hervé S, Bonin E *et al.* Spatio-temporal distribution and evolution of the A/H1N1 2009 pandemic virus in pigs in France from 2009 to 2017: identification of a potential swine-specific lineage. *J Virol* 2018;**92**:e00988-18.

Chastagner A, Hervé S, Quéguiner S *et al.* Genetic and antigenic evolution of European swine influenza A viruses of HA-1C (avian-like) and HA-1B (human-like) lineages in France from 2000 to 2018. *Viruses* 2020;**12**:1304.

Chepkwony S, Parys A, Vandoorn E *et al.* Genetic and antigenic evolution of H1 swine influenza A viruses isolated in Belgium and the Netherlands from 2014 through 2019. *Sci Rep* 2021;**11**:11276.

Chiapponi C, Prosperi A, Moreno A *et al.* Genetic variability among swine influenza viruses in Italy: data analysis of the period 2017–2020. *Viruses* 2021;**14**:47.

Choi YK, Lee JH, Erickson G *et al.* H3N2 influenza virus transmission from swine to turkeys, United States. *Emerg Infect Dis* 2004;**10**:2156–60.

Danecek P, Bonfield JK, Liddle J *et al.* Twelve years of SAMtools and BCFtools. *GigaScience* 2021;**10**:giab008.

Deblanc C, Queguiner S, Gorin S *et al*. Pathogenicity and escape to pre-existing immunity of a new genotype of swine influenza H1N2 virus that emerged in France in 2020. *Vet Res* 2024;**55**: 65.

Encinas P, Del Real G, Dutta J *et al*. Evolution of influenza A virus in intensive and free-range swine farms in Spain. *Virus Evol* 2022;**7**:veab099.

The European Commission. *European Union Law, Commission Delegated Regulation (EU) 2020/688*. 2019.

Gourreau JM, Kaiser C, Valette M *et al*. Isolation of two H1N2 influenza viruses from swine in France. *Arch. Virol* 1994;**135**:365–82.

Henritzi D, Peter Petric P, Sarah Lewis N *et al*. Surveillance of European domestic pig populations identifies an emerging reservoir of potentially zoonotic swine influenza A viruses. *Cell Host Microbe*, 2020;**28**:614–27.

Hervé S, Garin E, Calavas D *et al*. Virological and epidemiological patterns of swine influenza A virus infections in France: cumulative data from the RESAVIP surveillance network, 2011–2018. *Vet Microbiol* 2019;**239**:108477.

IFIP—Institut du Porc. *The Evolution of Pig Production in France*. 2023. https://www.pig333.com/articles/how-has-pig-production-evolved-in-france_19488/ (4 July 2024, date last accessed).

Janke BH. Clinicopathological features of Swine influenza. *Curr Top Microbiol Immunol* 2013;**370**:69–83.

Katoh K, Standley DM. MAFFT multiple sequence alignment software version 7: improvements in performance and usability. *Mol Biol Evol* 2013;**30**:772–80.

Koçer ZA, Jones JC, Webster RG. Emergence of influenza viruses and crossing the species barrier. *Microbiol Spectr* 2013;**1**:OH–0010–2012.

Lewis NS, Russell CA, Langat P *et al*. The global antigenic diversity of swine influenza A viruses. *Elife* 2016;**5**:e12217.

Ma W. Swine influenza virus: current status and challenge. *Virus Res* 2020;**288**:198118.

Massin P, Briand FX, Cherbonnel M *et al*. Detection of pandemic H1N1 in turkey breeders in France. In: *Proceedings VIIIth International Symposium on Turkey Diseases*, 27–29 May 2010, Berlin, Germany, 212–21, 2010.

Minh BQ, Schmidt HA, Chernomor O *et al*. IQ-TREE 2: new models and efficient methods for phylogenetic inference in the genomic era. *Mol Biol Evol* 2020;**37**:1530–4.

Minin VN, Bloomquist EW, Suchard MA. Smooth skyride through a rough skyline: Bayesian coalescent-based inference of population dynamics. *Mol Biol Evol* 2008;**25**:1459–71.

Nelson MI, Worobey M. Origins of the 1918 pandemic: revisiting the swine "Mixing Vessel" hypothesis. *Am J Epidemiol* 2018;**187**:2498–502.

Parys A, Vereecke N, Vandoorn E *et al*. Surveillance and genomic characterization of influenza A and D viruses in swine, Belgium and the Netherlands2019–2021. *Emerg Infect Dis* 2023;**29**: 1459–64.

Pol F, Quéguiner S, Gorin S *et al*. Validation of commercial real-time RT-PCR kits for detection of influenza A viruses in porcine samples and differentiation of pandemic (H1N1) 2009 virus in pigs. *J Virol Methods* 2011;**171**:241–7.

Portugal S, Cortey M, Tello M *et al*. Diversity of influenza A viruses retrieved from respiratory disease outbreaks and subclinically infected herds in Spain (2017–2019). *Transbound Emerg Dis* 2021;**68**:519–30.

Richard G. *gtrichard/influenza_sequences_toolbox: Influenza Sequences Toolbox 0.5*. Zenodo. 2024.

Richard G, Byrne A, and European Swine Influenza Network. *European Swine Influenza Network Report on Swine Influenza A Viruses Evolution and Diversity in Europe from October 2022 to September 2023*. Zenodo, 2024.

Rose N, Madec F. Occurrence of respiratory disease outbreaks in fattening pigs: relation with the features of a densely and a sparsely populated pig area in France. *Vet Res* 2002;**33**:179–90.

Sagulenko P, Puller V, Neher RA. TreeTime: maximum-likelihood phylodynamic analysis. *Virus Evol* 2018;**4**:vex042.

Schrauwen EJ, Fouchier RA. Host adaptation and transmission of influenza A viruses in mammals. *Emerging Microbes Infect*. 2014;**3**:e9.

Shen W, Le S, Li Y *et al*. SeqKit: a cross-platform and ultrafast toolkit for FASTA/Q file manipulation. *PLoS One* 2016;**11**:e0163962.

Shinde V, Bridges CB, Uyeki TM *et al*. Triple-reassortant swine influenza A (H1) in humans in the United States, 2005–2009. *New Engl J Med* 2009;**360**:2616–25.

Short KR, Richard M, Verhagen JH *et al*. One health, multiple challenges: the inter-species transmission of influenza A virus. *One Health* 2015;**1**:1–13.

Simon G, Larsen LE, Durrwald R *et al*. European surveillance network for influenza in pigs: surveillance programs, diagnostic tools and Swine influenza virus subtypes identified in 14 European countries from 2010 to 2013. *PLoS One* 2014;**9**:e115815.

Sooryanarain H, Elankumaran S. Environmental role in influenza virus outbreaks. *Annu Rev Anim Biosci* 2015;**3**:347–73.

Starick E, Fereidouni SR, Lange E *et al*. Analysis of influenza A viruses of subtype H1 from wild birds, turkeys and pigs in Germany reveals interspecies transmission events. *Influenza Other Respir Viruses* 2011;**5**:276–84.

Suchard MA, Lemey P, Baele G *et al*. Bayesian phylogenetic and phylodynamic data integration using BEAST 1.10. *Virus Evol* 2018;**4**:vey016.

te Beest DE, van Boven M, Hooiveld M *et al*. Driving factors of influenza transmission in the Netherlands. *Am J Epidemiol* 2013;**178**:1469–77.

Trebbien R, Bragstad K, Erik Larsen L *et al*. Genetic and biological characterisation of an avian-like H1N2 swine influenza virus generated by reassortment of circulating avian-like H1N1 and H3N2 subtypes in Denmark. *Virol J* 2013;**10**:290.

Vandoorn E, Leroux-Roels I, Leroux-Roels G *et al*. Detection of H1 swine influenza A virus antibodies in human serum samples by age group. *Emerg Infect Dis* 2020;**26**:2118–28.

Vincent A, Awada L, Brown I *et al*. Review of influenza A virus in swine worldwide: a call for increased surveillance and research. *Zoonoses Public Health* 2014;**61**:4–17.

Wagih O, Hancock J. ggseqlogo: a versatile R package for drawing sequence logos. *Bioinformatics* 2017;**33**:3645–7.

WOAH. Chapter 3.9.3. Influenza A viruses of swine. *Manual of Diagnostic Tests and Vaccines for Terrestrial Animals*, 13th edn. Paris, France: World Organisation for Animal Health, 2023.

Zell R, Groth M, Krumbholz A *et al*. Displacement of the Gent/1999 human-like swine H1N2 influenza A virus lineage by novel H1N2 reassortants in Germany. *Arch. Virol* 2020;**165**:55–67.

Zhang H, Li H, Wang W *et al*. A unique feature of swine ANP32A provides susceptibility to avian influenza virus infection in pigs. *PLoS Pathogens* 2020;**16**:e1008330.

Zhou B, Donnelly ME, Scholes DT *et al*. Single-reaction genomic amplification accelerates sequencing and vaccine production for classical and swine origin human influenza a viruses. *J Virol* 2009;**83**:10309–13.

Virus Evolution, 2025, 11(1), veae112 , DOI: https://doi.org/10.1093/ve/veae112, Advance Access Publication 14 December 2024, Research Article